Matrix Electron Nuclear Double Resonance Studies of the Proton Environment of the Radical in Natural and Solvent-Refined Coal

S. Schlick, P. A. Narayana, and Larry Kevan*

Contribution from the Department of Chemistry, Wayne State University, Detroit, Michigan 48202. *Received February 15, 1977*

Abstract: The radical in natural and solvent-refined coal (SRC) has been studied by electron nuclear double resonance (ENDOR) between room temperature and 30 K as a function of the microwave and radio-frequency field intensities. The observation of a strong proton matrix ENDOR line shows interaction of the coal radical with nearby protons. By simulating the matrix ENDOR line with a new, improved line shape model we conclude that the closest protons are situated at 2.6 ± 0.2 Å from the unpaired electron of the coal radical and that the average isotropic hyperfine coupling of these closest protons is 1.3 ± 0.3 MHz. The experimental variation of the matrix ENDOR line shape and intensity with microwave and radio-frequency field intensity is simulated well at lower microwave powers by the improved ENDOR line shape model although deviations occur at higher microwave power. The differences of the ENDOR signals for natural and solvent-refined coal are explained in terms of different electron and nuclear spin–lattice relaxation times, in line with the rather well-established assumption that the structures in both coals are similar.

Introduction

The nature of the electron spin resonance (ESR) signal obtained by heating or high-energy irradiation of natural products such as wood, sugar, and coal has been the subject of numerous investigations.[1] It has been suggested[2] that the ESR signals thus obtained are the same as those observed naturally in coals. The factors responsible for the ESR signal in untreated coal are believed to be associated with radiothermal or geothermal activity.[1] Carbon blacks, which exhibit this typical ESR signal, are used extensively in many industries such as rubber, plastics, and paints, and therefore there is considerable interest in their properties.

Because of their varied origin, natural coals contain variable amounts of elements such as oxygen, nitrogen, sulfur, and hydrogen. The ESR signal measured in natural coals and in irradiated or pyrolyzed (at temperatures lower than 900 °C) carbons is in most cases 4–9 G wide[3] and shows no resolved hyperfine structure.

Some insight into the structure of the coal and on the environment of the unpaired electron has been obtained by analysis of the variations in line widths and g values of different coals.

The line width is believed to be due to unresolved hyperfine interaction of the electron spin with hydrogen nuclei. Retcofsky et al.[3] have measured an increase in line width with the percentage of analyzed hydrogen in different coals.

The g-value range is 2.0027–2.0042 in most coals,[4] with the higher g values corresponding to coals with lower carbon content. This was interpreted as delocalization of the electron spin onto atoms with higher spin–orbit coupling constants such as N or S.

One way to obtain "clean" coal is by the solvent refining process. The pulverized raw coal is mixed with a high boiling point aromatic solvent, hydrogen is added, and the dissolution takes place at ~450 °C.[5] The solvent is then removed in a distillation column. The residue is the solvent-refined coal (SRC). Preliminary analytical techniques have been used to obtain details on the structure of SRC. The main conclusions are that the radical concentration is lower and the hydrogen concentration higher in SRC compared to raw coal.[5,6]

It is well known that the electron nuclear double resonance (ENDOR) technique is very helpful in elucidating hyperfine interactions not easily observable by ESR.[7] In single crystals this is generally true because of increased effective spectral resolution. In disordered systems, however, the hyperfine information must often be obtained by line shape analysis of the "matrix" ENDOR line occurring at the free nuclear frequency. For weak hyperfine interactions we have shown how analysis of the matrix ENDOR line can give a variety of structural information.[8]

In the present study we use matrix ENDOR to deduce the first details of the proton environment around the unpaired electron in natural and solvent-refined coal. Since the SRC sample gives strong ENDOR signals at room temperature it also serves as a convenient system to test the predictions of an improved matrix ENDOR model on the microwave and radio-frequency field dependence of the matrix ENDOR response.[9]

Experimental Section

Measurements were made on Pittsburgh no. 8 raw coal and the corresponding solvent-refined sample from a coal conversion pilot plant at Wilsonville, Ala., both kindly supplied to us by Dr. L. T. Taylor of the Virginia Polytechnic Institute and State University. It was stated that 99.5% of the SRC dissolves in tetrahydrofuran.

The ENDOR spectra were recorded on a Varian V-4500 electron spin resonance spectrometer interfaced with a Varian E-700 ENDOR unit. The radio-frequency (rf) field is pulsed at 6 kHz and the magnetic field is modulated at low frequency (40 Hz).

The microwave power was measured with a Hewlett-Packard HP 431 C powermeter. The microwave magnetic field H_1, in gauss, is given by the relation[10]

$$H_1^2 = 3.34 \times 10^{-4} P_w Q_L \qquad (1)$$

where P_w is the incident microwave power in watts and Q_L is the loaded Q of the cavity. For the ENDOR cavity $Q_L \simeq 3000$. Because of the inherent assumptions used in relationship 1, such as a point sample in the cavity center and critical coupling, the H_1 obtained is not highly accurate. However, as will be seen below, it is most important to know the relative values of H_1 at different microwave power levels accurately, rather than absolute values of H_1.

The maximum radio-frequency magnetic field (H_2) was estimated to be 5 G[10] and was measured from the induced voltage in a pick-up coil of known dimensions.

The electronic spin–lattice relaxation time T_{1e} was measured by the saturation–recovery technique with a time-domain X-band ESR spectrometer built in this laboratory.[11] Measurements were done with saturating pulses longer than the measured relaxation time to minimize complications due to cross relaxation.

0002-7863/78/1500-3322$01.00/0

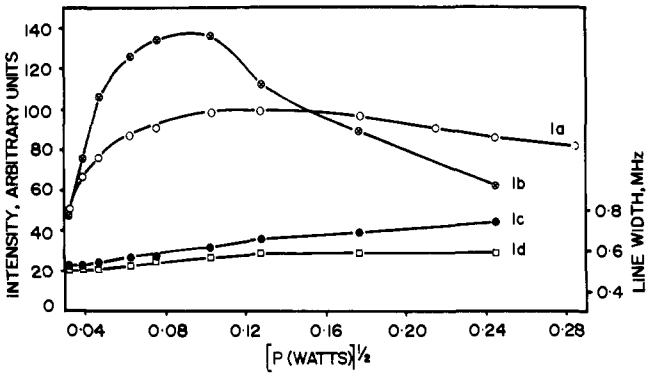

Figure 1. ESR spectral intensity (1a), ENDOR spectral intensity for H_2 = 5 G (1b), and ENDOR line width for H_2 = 5 G (1c) and for H_2 = 2.5 G (1d) as a function of (microwave power)$^{1/2}$ for SRC at room temperature.

Results

The unremarkable ESR spectrum of the SRC samples is a single, almost Lorentzian line, with a peak-to-peak width of about 7 G and g = 2.0034 at room temperature. The ESR power saturation curve is given in Figure 1a.

In the SRC sample strong matrix ENDOR signals around 14 MHz were observed at room temperature over the range of microwave power from 1 to 150 mW. This indicates interaction with hydrogen nuclei surrounding the unpaired electron. The ENDOR power saturation curve with H_2 = 5 G is given in Figure 1b. Line widths of the ENDOR line (at half maximum intensity, in MHz) as a function of the square root of microwave power are shown in Figure 1c (for H_2 = 5 G) and in Figure 1d (for $H_2 \simeq$ 2.5 G).

Line shapes and line widths at half maximum intensity of the ENDOR line change markedly with microwave power and typical spectra at various microwave power levels are shown in Figure 2.

It is obvious from these results that the shape, intensity, and widths of the matrix ENDOR lines observed are sensitive to both H_1 and H_2. Thus the maximum information can be obtained only from a model for the matrix ENDOR response that includes these two parameters.

The ESR line width of raw coal is ~6 G at room temperature. The signal in raw coal saturates much less than that in SRC at room temperature implying a shorter spin–lattice relaxation time for raw coal. Consequently, no ENDOR signals are seen in raw coal at room temperature. ENDOR is seen at lower temperatures between 110 and 160 K, however, with the best signal occurring near 150 K. A typical spectrum at a power level of 4 mW is shown in Figure 3. It is practically identical with the signal obtained at room temperature from SRC. Because of the poor signal/noise ratio, no systematic investigation of this matrix ENDOR signal as a function of microwave and radio-frequency power was undertaken.

Theory

The matrix ENDOR line is interpreted as due to predominantly dipolar interaction between the unpaired electron and the surrounding nuclei.[8,12-14] The matrix lines contain information about the delocalization of the unpaired electron. This information can be extracted by simulation of the matrix ENDOR line within the constraints of a model for the ENDOR response.

A matrix ENDOR line can be simulated as a function of two parameters: α, which is the half-width at half-height of the nuclear spin packet, and $\bar{a}$, which is the distance beyond which the interaction between the electron and the matrix nuclei is purely dipolar with no isotropic hyperfine contribution.

This simple model, useful as it is for a qualitative or at best

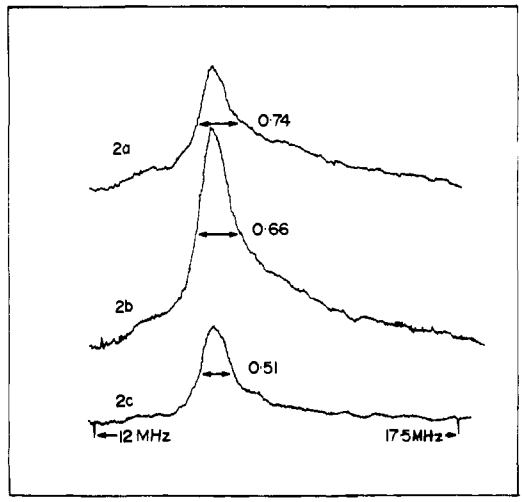

Figure 2. Matrix ENDOR lines for SRC at room temperature at different microwave power levels: 120 (2a), 34 (2b), and 2 mW (2c). Widths at half maximum intensity (in MHz) are indicated. Rf field is 5 G.

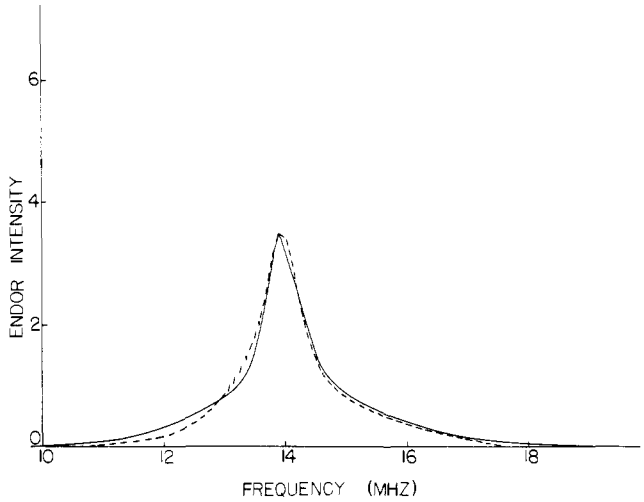

Figure 3. Experimental matrix ENDOR line at microwave power 6 mW for raw coal at 150 K (broken line) and calculated simulations (full line) with the following parameters: T_{1e} = 120 μs, T_{2e} = 1.2 μs, T_{1n}^{intra} = 0.6 s, T_{2M} = 90 μs, r_{min} = 2.6 Å, and a_{iso} = 1.3 MHz at distances less than 4 Å. The rf field is 2.5 G.

semiquantitative interpretation of matrix ENDOR, has obvious limitations which can be summarized as follows. It does not include various relaxation paths and it fails to account for the experimentally observed dependence of the matrix ENDOR line on the rotating components of the microwave and radio-frequency magnetic fields, H_1 and H_2. Hochman et al.[15] have formulated a model for ENDOR responses in single crystals which overcomes the above limitations and is based on a density matrix formalism. Narayana et al.[9] have used this approach to develop an improved matrix ENDOR line shape model which does depend on H_1 and H_2 as well as on the various relaxation rates in the spin system. With this improved matrix ENDOR model they were able to successfully simulate the matrix ENDOR response for trapped electrons in 2-methyltetrahydrofuran glass at 77 K and to determine the isotropic and anisotropic coupling constants to the nearest matrix protons.

We will use this improved matrix ENDOR model to analyze our results on the coal sample. The spin system has $S = \frac{1}{2}$ and $I = \frac{1}{2}$. We assume that the Hamiltonian has axial symmetry with an isotropic g factor and we neglect the nonsecular terms involving S_x and S_y. In general the ENDOR signal $\delta_\pm$ is given by

$$\delta_{\pm} = \frac{[\chi'' - \chi''(H_2 = 0)]H_1}{[\chi''(H_2 = 0)H_1]_{max}} \quad (2)$$

where $\chi''(H_2 = 0)H_1$ is the out-of-phase magnetization as measured by ESR. The final expression for the matrix ENDOR enhancement is[9]

$$\delta_{\pm} = \left(\frac{X^2}{1 + X^2}\right)^{1/2} \times \left[\left(\frac{1 + X^{-2}}{1 + X^{-2} - (1 - \alpha_{\pm})C(1 + Y_{\pm}^{-2})^{-1}}\right)^{1/2} - 1\right] \quad (3)$$

where X^2 is the product of the ESR transition probability, which involves H_1, and an effective T_{1e}; Y^2 is the product of the ENDOR transition probability, which involves H_2, and an effective T_{1n}; $\alpha_{\pm}$ is a function of the various relaxation parameters; and C is an overlap correction to correct for nuclear level population differences when the ESR transitions are closely spaced. The transition probabilities involve Lorentzian line shape functions characterized by T_{2e} and T_{2n}, electron and nuclear spin-spin relaxation times. T_{1e}^{eff}, T_{1n}^{eff}, and $\alpha_{\pm}$ are functions of the relaxation probabilities for electron spin flips, W_s, nuclear spin flips, W_n, and simultaneous electron and nuclear spin flips, W_x and $W_{x'}$. The explicit details have been given.[9]

The overlap correction, C, in eq 3 is based on Redfield's formulation[16] and is given by[9]

$$C = \frac{\Delta\omega^2}{\Delta\omega^2 + \gamma_e(H_1^2 + 2(\delta H)^2)} \quad (4)$$

where $\Delta\omega$ is the separation between the ESR transitions, γ_e is the electron gyromagnetic ratio, and δH is the Lorentzian spin packet half-width at half-height given by $\delta H = (\gamma_e T_{2e})^{-1}$. Previously,[9] we assumed that H_1 was large and determined δH, but this assumption gives poor agreement with the present experiments. Therefore, we have retained $\delta H = (\gamma_e T_{2e})^{-1}$ in the present simulations to compare with the H_1 range investigated experimentally.

For a disordered polycrystalline matrix the average ENDOR response is obtained by averaging over all orientations and summing the contributions from nuclei located at different distances from the umpaired electron according to

$$\delta = \int_{r_{min}}^{\infty} \langle \delta_+(r_i, \theta, \phi) + \delta_-(r_i, \theta, \phi) \rangle_{\theta} r^2 dr \quad (5)$$

In this model no assumptions about the strengths of H_1 and H_2 are made. The model also explicitly includes both direct and cross relaxation mechanisms and might provide a possibility of determining which relaxation mechanisms are operative in the system.

Matrix ENDOR lines can be simulated from this model from experimentally measured or estimated values of H_1, H_2, T_{2e}, T_{2n}, and the various relaxation probabilities and compared with experimental spectra to determine r_{min}, the distance of the closest nuclei to the unpaired electron, and a_{iso}, the average isotropic hyperfine interaction of the closest nuclei. In addition, the ENDOR response vs. H_1 and H_2 can be calculated to compare with experiment.

Spectral Simulation and Discussion

A. Solvent-Refined Coal. We will simulate the ENDOR spectra for the radical in solvent-refined coal under the following contraints. Experimental values of H_1, H_2, T_{1e}, and T_{2e} are used. The cross relaxation times, T_x and $T_{x'}$, are written in terms of T_{1e} by assuming that the cross relaxation arises due to the mixing of the energy states by hyperfine coupling.[9] The remaining parameters T_{1n}, T_{2n}, r_{min}, and a_{iso} are determined by fitting the simulated spectra to the experimental ones. We will find that it is possible to determine all of these parameters within rather narrow limits. We now discuss the determination and estimation of the various relaxation times.

The electron spin-lattice relaxation time was measured by the saturation recovery method and at room temperature it was found that $T_{1e} = 120 \pm 40$ μs.

We succeeded in measuring electron spin echoes[17] from the SRC sample between 18 and 160 K. The two pulse electron spin echo decays with a temperature-independent phase memory time of ~1.2 μs which we interpret as a reasonable approximation for T_{2e}. This value was used in the simulations.

The nuclear spin-spin relaxation time T_{2n} can be measured by nuclear magnetic resonance (NMR). We were not able to make such measurements on our samples, but we are guided by previous measurements on coal samples which are in the range of 10-120 μs.[18]

The formulation of the nuclear spin-lattice relaxation time must be treated carefully. We formulate it in two parts. The first part is the intrinsic nuclear relaxation in a diamagnetic matrix, T_{1n}^{intra}, which is independent on the unpaired electron-nuclear distance. The second part is the nuclear relaxation due to the presence of the unpaired electron which will depend strongly on the electron-nuclear distance, r. We assume that this relaxation is dominated by the electron-nuclear dipolar interaction modulated by electron spin relaxation. From the measured value of T_{1e} and considering contributions from the pseudosecular term of the dipolar interaction ($\propto S_z I_{\pm}$) only we have[9]

$$(T_{1n}^{para})^{-1} = \frac{9}{4} T_{1e}^{-1} \gamma_e^2 \gamma_n^2 \hbar^2 \sin^2\theta \cos^2\theta (2\pi\nu_p)^{-2} r^{-6} \quad (6)$$

where γ_e and γ_n are the electron and nuclear gyromagnetic ratios and ν_p is the proton resonance frequency in the applied field. The total nuclear relaxation time is then given by

$$(T_{1n})^{-1} = (T_{1n}^{intra})^{-1} + (T_{1n}^{para})^{-1} \quad (7)$$

T_{1n}^{intra} can, in principle, be measured by NMR. In coal samples, however, it is impossible to measure this parameter because the diamagnetic material is not available; the coal samples contain unpaired electrons. A reasonable estimate is possible from T_{1n}^{intra} measurements on model compounds, without unpaired electrons. A typical measured[19] model compound value is 700 ms at room temperature.

The value of a_{iso} should decrease with distance for a spherically symmetric unpaired electron distribution. Based on previous determinations of matrix proton coupling constants from other studies[20] we have assumed that a_{iso} can be neglected beyond 4 Å and expect that $a_{iso} \approx 1$ MHz between 3 and 4 Å and >1 MHz at <3 Å.

Simulation of the matrix ENDOR line at the microwave power which gives the maximum ENDOR response (4 mW) leads to the good fit with experiment shown in Figure 4 for r_{min} = 2.6 Å and a_{iso} = 1.3 MHz at distances <4 Å; the other parameters are given in the figure caption.

Although there are four parameters to be chosen, the simulations show that these parameters affect the calculated ENDOR line in quite different ways. As a general statement we conclude that it is not difficult to simulate the *central portion* of the spectrum but the simulation of the *entire* spectrum including the wings strongly narrows the choice of parameters. Moreover, the different parameters affect the calculated ENDOR line in a different manner.[9] After having calculated numerous spectra with different parameters we have confidence that, within certain limits which will be given below, the choice of parameters in Figure 4 is reasonably unique.

As a further check of the choice of parameters, we tried to simulate the entire range of matrix ENDOR lines obtained as

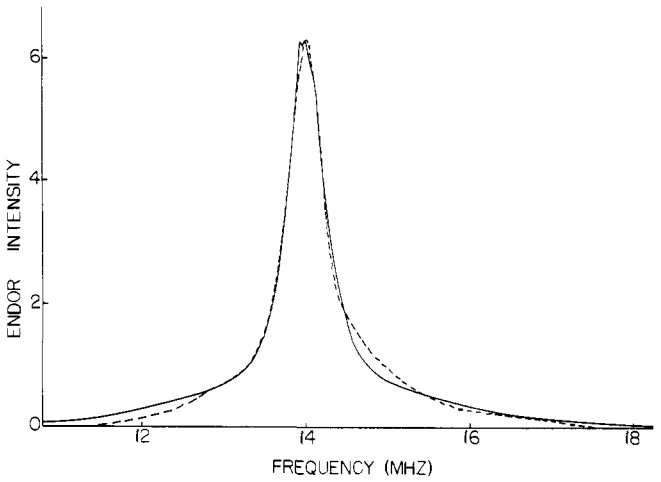

Figure 4. Experimental matrix ENDOR line at microwave power 4 mW for SRC sample at room temperature (broken line) and simulated line (full line) with the following parameters: $T_{1e} = 120\ \mu s$, $T_{2e} = 1.2\ \mu s$, $T_{1n}^{intra} = 0.40$ s, $T_{2n} = 90\ \mu s$, $r_{min} = 2.6$ Å, and $a_{iso} = 1.3$ MHz at distances less than 4 Å. The rf field is 2.5 G.

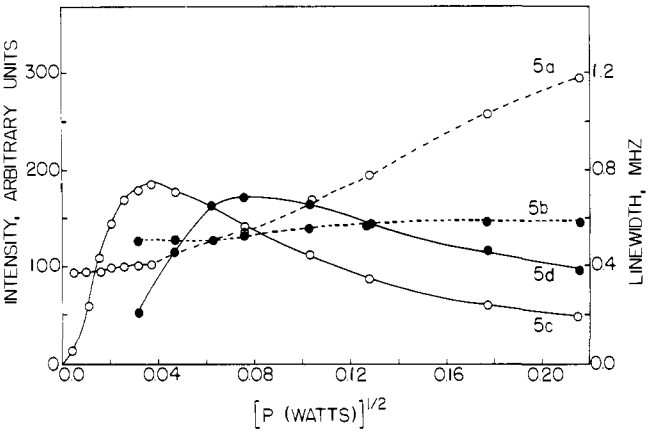

Figure 5. Matrix ENDOR line width and intensity for SRC sample at room temperature as a function of $P^{1/2}$, where P is the microwave power with $H_2 = 2.5$ G: (5a) calculated line width, (5b) experimental line width, (5c) calculated intensity, (5d) experimental intensity. Curves 5a and 5c were calculated with the following parameters: $T_{1e} = 120\ \mu s$, $T_{2e} = 1.2\ \mu s$, $T_{1n}^{intra} = 0.4$ s, $T_{2n} = 90\ \mu s$, $r_{min} = 2.6$ Å, and $a_{iso} = 1.3$ MHz for distances less than 4 Å.

a function of the microwave and radio-frequency field intensities.

Experimental variation of the radio-frequency field H_2 between 2 and 5 G has no appreciable effect on the matrix ENDOR line intensity, shape, and width (see Figures 1c and 1d). In most cases the line width was slightly higher at higher values of H_2 and spectra were well simulated with basically the same parameters. For $H_2 = 5$ G, T_{1n}^{intra} was decreased by 30% to 0.3 s for a better fit compared to $T_{1n}^{intra} = 0.4$ s at $H_2 = 2.5$ G.

Figure 5 shows experimental and simulated line widths and intensities as a function of the microwave power with $H_2 = 2.5$ G. Simulations were done with the set of parameters used for the simulation of the line at maximum ENDOR intensity (Figure 4).

The calculated and experimental intensities as a function of microwave power have a similar shape but maxima occur at different values of the microwave power. In view of the great difficulties usually encountered with calculations of ENDOR spectral intensities in general and ENDOR intensities in particular, the agreement is judged to be satisfactory.

The calculated and simulated line widths are within 0.1 MHz for microwave powers up to the region of the maximum ENDOR response. At higher microwave powers the simulated line width increases markedly while the experimental line width remains approximately constant. By slightly varying the parameters within the following reasonable ranges $T_{1n}^{intra} = 0.35 \pm 0.05$ s, $T_{2n} = 90 \pm 10\ \mu s$, $a_{iso} = 1.3 \pm 0.3$ MHz, and $r_{min} = 2.6 \pm 0.02$ Å, the agreement between calculated and simulated line widths at microwave powers up to the maximum ENDOR response is improved to within 0.03 MHz. While the similarity of calculated and experimental linewidths at low and medium microwave power is gratifying, the discrepancy at high microwave power is somewhat of a puzzle. One possible explanation is that the assumpiton of H_1-independent relaxation parameters becomes incorrect at high power levels and thus the theoretical formulation used here should be modified.

It is worthwhile to note that the value of experimental H_1 is very important and the accuracy of H_1 measurements is probably no better than a factor of 2. If H_1 is lower than that calculated from the measured value of the microwave power and the cavity characteristics, the calculated data in Figure 5 are shifted to higher $P^{1/2}$ values and the agreement with the experimental data is better.

B. Raw Coal. The shape of the matrix ENDOR line in raw coal at 150 K is similar to the matrix ENDOR line of SRC at room temperature, but the matrix ENDOR width at half-height is 0.85 MHz in raw coal compared to 0.55 MHz in SRC. Recall that we could not see ENDOR in raw coal at room temperature, presumably because of a too short T_{1e}. We did not directly measure T_{1e} in raw coal, but we can estimate from the power saturation curves that T_{1e} in raw coal near 150 K is similar to T_{1e} in SRC at room temperature. Therefore, we have made simulations for the matrix ENDOR in raw coal using the same parameters as for SRC except for T_{1n}, which we expect to be longer at the lower temperature of the ENDOR measurements in raw coal. Figure 3 shows that a satisfactory simulation for raw coal is obtained on this basis with $T_{1n}^{intra} = 0.6$ s which is twice as long as the T_{1n}^{intra} used for the SRC simulation. These results imply that the unpaired electron environments are similar in raw coal and solvent-refined coal.

The shorter T_{1e} in raw coal compared to SRC at room temperature may be due to cross relaxation contributions to the effective T_{1e} since the radical concentrations and perhaps the impurity levels are higher in raw coal.

Conclusions

One of the objectives of this study was to shed more light on the nature of the unpaired electron in SRC and raw coal. Although we cannot give a detailed description of the site of the electron spin, we can conclude:

(1) The very observation of a proton matrix ENDOR line shows interaction of the electron with nearby protons. To our knowledge this is the first direct observation of magnetic interaction with surrounding nuclei in coal that has been reported.

(2) From simulation of the matrix ENDOR line we can conclude that the closest protons are situated at a distance of 2.6 ± 0.2 Å from the unpaired electrons and that the average isotropic hyperfine coupling of these closest protons is 1.3 ± 0.3 MHz.

The detailed structure of coal is still unknown. Some structures have been proposed in which most of the carbon atoms are in highly substituted aromatic rings[21,22] which contain two or three benzene rings. It appears that most hydrogens are not attached directly to aromatic carbons. It is reasonable to assume that the unpaired electron in coal is stabilized by and delocalized onto the aromatic rings. Then the value of 2.6 Å for the distance of the closest protons to the radical site indicates that the protons interacting with the

unpaired electron are twice removed from the aromatic rings and this is in agreement with the small isotropic hyperfine splitting, 1.3 MHz, for these closest protons. Ring protons in polynuclear hydrocarbons such as anthracene and tetracene have a minimum splitting of 3 MHz. Such large splittings have not been observed in the ENDOR spectra of SRC and raw coal.

This study has also helped to evaluate the range of applicability of the new improved model for the matrix ENDOR response in disordered systems.[9] The experimental variation of line shape, line width, and intensity of the matrix ENDOR line is reproduced very well as a function of both the microwave and radio-frequency field intensities for microwave powers up to that which gives the maximum ENDOR response. The deviation of the experimental spectra from the simulated ones at high microwave power may be related to the approximation that the relaxation parameters are independent of the microwave field. The satisfactory agreement of the theory with the experimental spectra at low and medium microwave powers lends confidence in its ability to give new and useful structural information about paramagnetic species in disordered solids.

Acknowledgment. This work was supported by the U.S. Army Research Office and the Wayne State University Computing Center. We thank Dr. L. T. Taylor for drawing our attention to this coal sample and Drs. D. Becker and J. Michalik for the measurement of T_{1e}.

References and Notes

(1) R. S. Alger, "Electron Paramagnetic Resonance: Techniques and Applications", Wiley-Interscience, New York, N.Y., 1968, p 416, and references cited therein.
(2) J. Uebersfeld, A. Etienne, and J. Combrisson, *Nature (London)*, **174**, 614 (1954).
(3) H. L. Retcofsky, G. P. Thompson, R. Raymond, and R. A. Friedel, *Fuel*, **54**, 126 (1975).
(4) H. L. Retcofsky, J. M. Stark, and R. A. Friedel, *Anal. Chem.*, **40**, 1699 (1968).
(5) D. L. Wooton, H. C. Dorn, L. T. Taylor, and W. M. Coleman, *Fuel*, **55**, 224 (1976).
(6) L. T. Taylor, private communication.
(7) See, for instance, L. Kevan and L. D. Kispert, "Electron Spin Double Resonance Spectroscopy, Wiley-Interscience, New York, N.Y., 1976.
(8) (a) J. Helbert, L. Kevan, and B. L. Bales, *J. Chem. Phys.*, **57**, 723 (1972); (b) J. Helbert and L. Kevan, *ibid.*, **58**, 1205 (1973); (c) B. L. Bales, R. N. Schwartz, and L. Kevan, *Chem. Phys. Lett.*, **22**, 13 (1973); (d) R. N. Schwartz, M. K. Bowman, and L. Kevan, *J. Chem. Phys.*, **60**, 1690 (1974); (e) H. Hase, F. Q. H. Ngo, and L. Kevan, *ibid.*, **62**, 985 (1975); (f) J. N. Helbert, B. E. Wagner, E. H. Poindexter, and L. Kevan, *J. Polym. Sci., Polym. Phys. Ed.*, **13**, 825 (1975).
(9) P. A. Narayana, M. K. Bowman, D. Becker, L. Kevan, and R. N. Schwartz, *J. Chem. Phys.*, **67**, 1990 (1977).
(10) J. Helbert, Ph.D. Thesis, Wayne State University, 1972.
(11) (a) M. K. Bowman, Ph.D. Thesis, Wayne State University, 1975; (b) M. K. Bowman and L. Kevan, *J. Phys. Chem.*, **81**, 456 (1977).
(12) J. S. Hyde, G. H. Rist, and L. E. G. Eriksson, *J. Phys. Chem.*, **72**, 4269 (1968).
(13) D. S. Leniart, J. S. Hyde, and J. C. Vedrine, *J. Phys. Chem.*, **76**, 2079 (1972).
(14) J. C. Vedrine, J. S. Hyde, and D. S. Leniart, *J. Phys. Chem.*, **76**, 2087 (1972).
(15) V. L. Hochman, V. Ya. Zevin and B. D. Shanina, *Fiz. Tverd. Tela*, **10**, 337 (1968); *Sov. Phys.-Solid State (Engl. Trans).*, **10**, 269 (1968).
(16) A. G. Redfield, *Phys. Rev.*, **98**, 1787 (1955).
(17) P. A. Narayana, D. Becker, and L. Kevan, *J. Chem. Phys.*, in press.
(18) B. C. Gerstein, C. Chow, R. G. Pembleton, and R. C. Wilson, *J. Phys. Chem.*, **81**, 565 (1977).
(19) T. Yokono and Y. Sanada, private communication.
(20) K. Toriyama, K. Nunome, and M. Iwasaki, *J. Chem. Phys.*, **64**, 2020 (1976).
(21) D. L. VanderHart and H. L. Retcofsky, *Fuel*, **55**, 202 (1976).
(22) G. A. Mills, *Ind. Eng. Chem.*, **61**, 6 (1969).

Pressure Saturation of the Collisional Quenching of the $^3B_1$ State of SO_2

S. J. Strickler* and R. Neil Rudolph

Contribution from the Department of Chemistry, University of Colorado, Boulder, Colorado 80309. *Received August 19, 1977*

Abstract: Direct measurements are reported of the lifetime of the $^3B_1$ state of SO_2 at pressures from 8 to 1300 Torr, and in the presence of N_2, CO_2, and H_2O at varying pressures. It is shown that the collisional quenching saturates at higher pressures, approaching a limiting rate of about 1.3×10^6 s^{-1}. Two models are proposed to account for this effect: one a theory of radiationless transitions, and one a kinetic scheme involving other triplet states. The models predict different pressure dependences. The data favor the kinetic model, but are not good enough to distinguish definitely between the two.

I. Introduction

The spectra and lifetime of the $^3B_1$ state of sulfur dioxide have been of interest for some time. One reason is that this state is probably involved in atmospheric photochemistry of some importance.[1,2] Another reason is that the SO_2 molecule and this state in particular have been important in the development of theories of radiationless transitions in small molecules.[3-6]

The collisional quenching of the $^3B_1$ state by ground-state SO_2 and a number of other gases has been measured. These have generally been discussed in terms of the following types of processes:

$$^3SO_2 \xrightarrow{k_p} SO_2 + h\nu \quad (1)$$

$$^3SO_2 + M_i \xrightarrow{k_{qi}} SO_2 + M_i \quad (2)$$

In some studies at low pressures a pressure-independent nonradiative decay

$$^3SO_2 \xrightarrow{k_{nr}} SO_2 \quad (3)$$

has also been considered,[3] although other studies[7,8] have indicated it to be less important and theoretical considerations suggest that there should be no such process at the limit of zero pressure. In addition, some gases react chemically with the $^3B_1$ state of SO_2, and equations must be included to describe the

0002-7863/78/1500-3326$01.00/0